Environmental Technology & Innovation 32 (2023) 103391

Contents lists available at ScienceDirect

Environmental Technology & Innovation

journal homepage: www.elsevier.com/locate/eti

The ability of biochars from cookstoves to remove pharmaceuticals and personal care products from hospital wastewater

Brigitte Mukarunyana [a,c], Christoffer Boman [b], Telesphore Kabera [d], Robert Lindgren [b], Jerker Fick [a,*]

[a] Department of Chemistry, Faculty of Science and Technology, Umeå University, SE-901 87 Umeå, Sweden
[b] Department of Applied Physics and Electronics, Umeå University, SE-901 87 Umeå, Sweden
[c] Department of Chemistry, College of Science and Technology, University of Rwanda, P.O. Box 3900, Kigali, Rwanda
[d] School of Engineering, College of Science and Technology, University of Rwanda, P.O. Box 3900, Kigali, Rwanda

ARTICLE INFO

Keywords:
Hospital wastewater
PPCPs
Feedstock
Biochar cookstove
Removal rate

ABSTRACT

Adequate treatment of wastewater to remove micropollutants constitutes a major concern globally. Despite this, large volumes of untreated wastewater are released into the environment, mainly due to the cost involved. Biochars have been suggested to have the potential to remove pharmaceuticals and personal care products (PPCP) from wastewater, but, adsorption potential needs to be investigated further. Production of biochars should also preferably be sustainable and based on low-cost materials. This study investigated the ability of nine biochars produced in three cookstoves and from three feedstocks. All biochars were characterized and then applied in adsorption experiments, based on authentic hospital effluent. Our analytical method included 32 pharmaceuticals and personal care products, and 28 of these were detected and quantified in hospital wastewater effluent samples. Some PPCP were present in relatively high concentrations (more than 24 μg/L). Adsorption experiments showed that the biochars used in the investigation had average removal rates (RR) ranging from 14.2% to 65.5%. Removal rates also varied between and within cookstoves and feedstock. Although cookstove biochars with a low surface area in this study generally showed lower removal rates, results from surface characterization were not detailed enough to correlate the physicochemical properties of the pollutants with the adsorption. Further characterizations are therefore needed to point out the most important parameters involved in PPCP adsorption on cookstove biochars.

1. Introduction

Humans and animals consume pharmaceuticals to neutralize pathogens and control disease (Ram et al., 2020). Most of the consumed pharmaceutical is excreted either in a non-metabolized form or as metabolites with similar or different properties to the original compounds. These pollutants then enter the aquatic environment system via wastewater flows. Therefore, adequate treatment of wastewater is crucial to mitigate the environmental impact of pharmaceuticals. The occurrence of pharmaceuticals and personal

* Corresponding author.
E-mail address: jerker.fick@umu.se (J. Fick).

https://doi.org/10.1016/j.eti.2023.103391
Received 3 July 2023; Received in revised form 25 September 2023; Accepted 4 October 2023
Available online 6 October 2023

care products (PPCP) in water systems has an impact on water quality worldwide since they have ecotoxicological effects and increase antimicrobial resistance (Fekadu et al., 2019; Shin et al., 2021; Wilkinson et al., 2022). Currently, the pharmaceutical industry is growing by 6.5% each year, producing an ever-increasing variety of pharmaceutical substances (OECD, 2019). Changing demographics in developing countries, an increasingly elderly population in developed countries (Reis et al., 2019), and the establishment of food security strategies in intensifying agriculture means there is unlikely to be a deceleration in pharmaceutical consumption in the coming years (OECD, 2019; Wilkinson et al., 2022). Most pharmaceuticals are released from households, but there are also some hot spots, e.g., hospitals and production and formulation facilities. Hospitals are especially interesting since the consumption of pharmaceuticals per person is high and the levels of PPCP in untreated hospital effluent are among the highest detected levels in the world (Al-Maadheed et al., 2019; Aydin et al., 2019; Azuma et al., 2019; Deguenon et al., 2022; Ram et al., 2020; Vaudreuil et al., 2022).

To treat wastewater effluent, many hospitals apply conventional treatment techniques based on physicochemical and biological processes to remove solids, organic pollutants and nutrients. However, such methods have been reported to be ineffective (Schwendicke et al., 2016) as they require energy to add oxygen into the system to generate aerobic conditions for bacteria (Antal and Grønli, 2003; Domingues et al., 2017). Moreover, it has been argued that conventional treatment processes may not be able to completely remove PPCPs from wastewater (Cukierman et al., 2019; Domingues et al., 2017; Duku et al., 2011; Melvin and Leusch, 2016; Zhang et al., 2020). Adsorption has been suggested as a promising method to remove PPCPs from aqueous solutions because it can be easily achieved, efficient and low-cost technology (Chauhan et al., 2022; Kim et al., 2020; Shin et al., 2020). Various adsorbents (e.g., activated carbon, nanoparticles, clays, biochars, etc.) have been tested and shown to effectively remove PPCPs from wastewater. Recently, activated carbon was demonstrated to successfully adsorb PPCP (Bahamon, Vega, 2017; Piel et al., 2013; Shin et al., 2021). However, it was argued that it may not be economically efficient to use activated carbon (Dinesh Mohan et al., 2014), especially in developing regions like sub-Saharan Africa, because of its high cost (Patel et al., 2021; Posadas et al., 2014). Biochars are therefore prime candidates with high potential for application in developing countries because as adsorbents they are easy to produce and the raw materials used are low-cost and locally sourced (Mohan et al., 2011; Patel et al., 2019; Qiu et al., 2021). Biochars are solid materials generated during the thermochemical treatment of biomasses under a limited oxygen concentration via a process called pyrolysis (López-Cano et al., 2018; Mojiri et al., 2020; Skoulou et al., 2008). They can be produced from various biomasses, such as agricultural wastes, household solid wastes, animal wastes, wood wastes, etc. (Duku et al., 2011; Gao et al., 2015). Their characteristics vary depending on the type of biomass converted and the operating conditions used during production (Ferraro et al., 2021; Ippolito et al., 2020; Qiu et al., 2021). In the context of sub-Saharan Africa agriculture is the main income activity resulting in the production of agricultural biomasses like peels, pulps, husks, crop residues, etc. Although dried agricultural biomass is traditionally used in cooking, an important quantity of it is considered waste and an appropriate protocol for their disposal is not yet clearly established increasing challenges in waste management in that region. By using cookstoves that pyrolysed biomass, the heat or energy for cooking is generated and carbonaceous materials or biochars resulting from that pyrolysis are produced as well (Sundberg et al., 2020). These biochars can have various applications including wastewater treatment as adsorbents (Mohan et al., 2011). This is a sustainable way of reducing waste streams and valorizing agricultural biomass by transforming what was considered waste into raw materials. Although many studies have suggested that biochars are suitable adsorbents for removing contaminants from aqueous solutions or soil, current data are inconsistent. This may be due to the different feedstock materials and operational conditions used to produce biochars, as well as the applied techniques to investigate their adsorption abilities, and the types of analytes (Qiu et al., 2021; Qambrani et al., 2017; Tomczyk et al., 2020). In addition, the evaluation of biochars in the wastewater treatment domain requires many analytes having different chemical properties and applying realistic conditions like using authentic wastewater and affordable instrumentation for biochar production which make biochars cost-effective adsorbents.

The aim of this study was to investigate, in terms of removal rates, the ability of biochars produced by cookstoves to adsorb pharmaceuticals and personal care products from hospital wastewater. The study emphasized the sustainable waste management approach in combination with relevant adsorption experiments based on authentic hospital wastewater. To date, only a few studies have been published with these. As a result, three important aims of this study were:

(1) To Apply an analytical method with a wide range of analytes, which provides real measurements of the ongoing release of pharmaceuticals and personal care products from hospitals, the first of this kind in Rwanda and one of few from Africa
(2) To perform adsorption of pharmaceuticals and personal care products on biochars produced by cookstoves and from different feedstocks
(3) To introduce a novel evaluation of the removal rates emphasizing chemicals which have the potential to affect aquatic wildlife

2. Materials and methods

2.1. Chemicals

Methanol for standard solutions was of HPLC grade and purchased from Fisher Chemicals (Loughborough, UK). Hypergrade acetonitrile and methanol (LiChrosolv) for LC-MS were both purchased from Merck (Darmstadt, Germany). Formic acid (Fluka), as an additive eluent, was purchased from Sigma–Aldrich (Steinheim, Germany). Ultrapure water was supplied from a Merck Millipore Advantage A10 system equipped with a Q-Pod unit. All standards and labelled standards were of analytical grade (> 95%). Details are given in Supplementary material Table S1.

2.2. Study area and sampling

Wastewater samples were collected from the University Teaching Hospital of Kigali (CHUK), which is the largest referral hospital in Rwanda, situated in Nyarugenge District in the city centre of Kigali, Rwanda. At the time of the study, it had about 519 beds and approximately receives 1000 patients per day of which 400 are hospitalized. It has around 800 employees. Wastewater from different services of the hospital is collected in tanks where it undergoes treatment under anaerobic conditions, the resulting liquid is transferred to another open tank where aeration and disinfection by chlorine take place before being discharged. Effluents from CHUK enter Gitega, a stream that is directly connected to the CHUK wastewater treatment plant outlet, which later connects with Mpazi, a large public stream, which in turn discharges into the Nyabugogo River. Samples were taken of influent (INF) and effluent (EFF), i.e., wastewater collected at the inlet and outlet of the wastewater treatment plant of CHUK, respectively. Samples were taken twice a day for one week on three days (Monday, Wednesday and Friday) each morning at 9 a.m. after cleaning activities and at 3 p.m. each time, 3 consecutive samples were taken with an interval of 30 min between each take. Samples on the same day were mixed to obtain one daily composite sample of INF and one of EFF, resulting in six samples in total (n = 3 for INF and EFF). The samples were kept at – 18 °C until analysis.

2.3. Pre-treatment and LC-MS/MS analysis

Samples were thawed at room temperature and centrifugated at 3500 rpm for 5 min. After centrifugation, 5 mL of each sample was spiked with 5 ng of each internal standard. On-line SPE was carried out using a Dionex UltiMate 3000 UHPLC system consisting of two LC pumps (Ultimate LPG 3400 SD quaternary pump and HPG 3400RS binary UHPLC pump), an Accela Open autosampler (Thermo Scientific), an online SPE column (Waters, Oasis HLB, 2.1 ×20 mm, 15 μm) and an analytical column (Thermo Scientific Hypersil GOLD, 50 ×2.1 mm, 5 μm) equipped with a pre-column (Hypersil GOLD, 10 ×2.1 mm, 3 μm). The column compartment was kept at 25 °C. Chromeleon Xpress (Thermo Scientific) was used to control the UHPLC system. Samples were injected onto a 1 mL loop and transferred to the online SPE column by the quaternary pump using 0.1% formic acid in acetonitrile as eluent. After 70 s, the autosampler valve was switched and the binary pump started elution from the online SPE column through the analytical column using a gradient consisting of (A) 0.1% formic acid in Milli-Q water, and (B) 0.1% formic acid in acetonitrile. The UHPLC system was connected to a TSQ Quantiva triple quadrupole mass spectrometer (Thermo Scientific) equipped with a heated electrospray ionization ion source operating in positive mode. The resolution of both quadrupoles was 0.7 FWHM. The following conditions were used: spray voltage 3500 V, sheath gas 40 arbitrary units, sweep gas 0 arbitrary units, ion transfer tube temperature 350 °C, and vaporizer temperature 338 °C. To control the mass spectrometer and perform data analysis, Xcalibur (Thermo Scientific) was used. Two MS/MS transitions, one for quantification and one for qualification, were monitored for all analytes. MS/MS transitions, corresponding collision energies, tube lens voltages, associated internal standards and limit of quantification, and LOQ for each analyte are shown in Table S2 of the Supplementary Material.

2.4. Biochar preparation

Three feedstocks were considered in this project: one forestry residue (softwood (SW)) and two agro-industrial residues (bagasse (BG) and coffee husks (CH)). All fuels were pelletized into Ø8 mm pellets. Biochars were prepared using three types of improved cookstoves: two natural draft gasifier stoves (N1 and N2) and one forced draft gasifier stove (F). All stoves were classified as top-lit-up LUD) stoves, whereby a batch of fuel is filled in a canister and lit from the top. The working principle of these stoves was air staging, where a partial airflow (primary air) entered the bottom of the canister to provide enough oxygen to maintain the gasification of the fuel. The remaining air (secondary air) needed for complete combustion was introduced slightly above the fuel bed. N1 had a relatively short distance between the secondary air inlet and the exit of the stove, creating a lower natural draft through the stove compared with N2, which had a longer combustion zone between the fuel bed and the exits of the stove. Thus, the chimney effect generated higher primary and secondary airflow through the N2 cookstove. The forced draft gasifier had a fan forcing the air into the stove, giving better control of the airflow through the stove. Each fuel and stove combination generated in total nine different biochar samples (i.e., N1SW, N1BG, and N1CH; N2SW, N2BG, and N2CH; FSW, FBG and FCH), which were characterized and used for adsorption tests.

2.5. Biochar characterization

2.5.1. DRIFTS analysis and Raman spectroscopy

Diffuse reflectance infrared Fourier transform spectroscopy (DRIFTS) and Raman spectroscopy analysis was carried out to determine the chemical functional groups on the surface of the biochar samples. To perform DRIFTS,10 mg of biochar was added to 390 mg of KBr (Merck, Darmstadt, Germany) used for FTIR spectroscopy, and they were manually ground together in an agate mortar. Spectra were recorded under vacuum conditions of diffuse reflectance using a Bruker IFS 66 v/S FTIR spectrometer (Bruker Optik GmbH, Ettlingen, Germany). Data were collected from 400 to 4000 cm^{-1} at a resolution of 4 cm^{-1}. Raman analysis was performed on samples in glass vials using a Bruker Bravo spectrometer over the full range of automatic settings. To process the data, the spectra were cut from 300 to 1900 cm^{-1}, a normalization vector was used in the range 900–1700 cm^{-1}, and smoothing was performed with the Savitzky–Golay algorithm, 13 points. All processing was carried out in OPUS, version 7.8, using the built-in functions. All protocols were as described by Gorzsás and Sundberg (2014). Analysis of DRIFTS spectra was performed using an online IR spectrum table provided by Sigma Aldrich.

2.5.2. Surface area characterization

The surface area and pore size of biochars were investigated using adsorption-desorption of nitrogen and calculated by applying the Brunauer-Emmett-Teller method described in Naderi (2015); Thommes et al. (2015).

2.5.3. Elemental analysis

X-ray photoelectron spectroscopy (XPS) analysis was utilized to determine the atomic percentage of chemical elements in biochars. Using a clean spatula, a powdered biochar sample was pressed into a pellet on a sample holder. Spectra were recorded using a monochromatic source electron spectrometer (Kratos Axis Ultra DLD) operated at 120 W. Analyzer pass energy of 160 eV and 20 eV contributed to obtaining the wide spectra and photoelectron lines respectively. The scale of binding energy was referenced against that of aliphatic carbon (C1s line), which was fixed at 285 eV. Spectra were processed using Kratos software.

2.6. Adsorption experiments

Adsorption experiments were performed at 20 °C in triplicate using 50 mg of biochar (± 2.5 mg) and 10 mL (± 0.01 mL) of treated hospital effluent in 15 mL plastic tubes. The biochar was weighed, the effluent sample was added to the tube and the mixture was agitated for 30 min at room temperature (22 °C). Experiments were terminated by centrifuging the samples for 5 min (4500 rpm). 5 mL of the supernatant was transferred to a vial and internal standards were added. Samples were analyzed within 24 h. Triplicate blank samples (Milli-Q water, no biochar) were also prepared and analyzed. Adsorption of analytes to the tube walls was investigated by a triplicate tube adsorption test (1 μg/L of each analyte added in Milli-Q water, no biochar). Hospital effluent used to calculate removal rates in the experiments was also agitated for 30 min in test tubes (no biochar added).

2.7. Data processing

Average (Av) and relative standard deviation (RSD) values were calculated using common statistical methods in Microsoft Excel 2016. ANOVA tests were conducted using Microsoft Excel to investigate differences between the removal rates of biochars produced in the same stove but from different feedstocks and biochars from the same feedstock but processed by different stoves. The comparison was performed based on *p*-values with the level of significance set at 0.05. The removal rate (RR) was calculated from Eq. 1, where C_{initial} and C_{final} are the initial (before adsorption experiment) and final (after adsorption experiment) concentrations of a PPCP, respectively.

$$RR(\%) = \frac{\text{C}initial - \text{C}final}{\text{C}initial} \times 100\% \quad (1)$$

3. Results and discussion

3.1. Hospital wastewater analysis

In total, 28 PPCPs were detected in hospital wastewater from the University Teaching Hospital of Kigali (CHUK) and quantified: 25 pharmaceuticals, 2 herbicides/pesticides and 1 stimulant. The 25 pharmaceuticals belonged to 14 therapeutic groups; 2 analgesics (A), 2 nonsteroidal anti-inflammatory drugs (NSAID), 3 antimalarial drugs (AMD), 3 antiretrovirals (ARV), 3 psycholeptics (PL) and 7 antibiotics (ATB), namely ciprofloxacin, clindamycin, erythromycin, levofloxacin, metronidazole, sulfamethoxazole and trimethoprim. Other groups with one analyte each were as follows: a hypertension drug (HD), a stimulant (S), an anti-ulcer drug(AUD), a plasticizer (P), an insecticide (I), an antimycotic (AM), a local anaesthetic (LA) and gastrointestinal drug (GD. The high occurrence of ATB, NSAIDs and analgesics was reported in a study analyzing effluents from different hospitals in Iran (Santos et al., 2013) in addition, they are the most prescribed pharmaceuticals indicated by a study carried out in Canada on 30 hospitals and 6 municipal effluents (Vaudreuil et al., 2022) and reported in different studies performed worldwide (Aydin et al., 2019; Azuma et al., 2019; Deguenon et al., 2022). The average concentrations ($n = 3$) of the analyzed PPCPs in INF ranged from <LOQ (e.g., carbamazepine) to 244000 ng/L (paracetamol). In EFF, average ($n = 3$) concentrations ranged from 12.5 (artemether) to 15000 ng/L (paracetamol). Twelve pharmaceuticals in INF and 11 in EFF had concentrations higher than 1 μg/L. The five analytes with the highest concentrations in INF were paracetamol (NSAID), caffeine (Stimulant), abacavir (ARV), lignocaine (A), and ciprofloxacin (ATB) (concentrations of 244000 ng/L, 38300 ng/L, 14700 ng/L, 13100 ng/L, and 8730 ng/L, respectively). In EFF, the five highest average concentrations were for paracetamol, lignocaine, erythromycin, ciprofloxacin (ATB), and tramadol (A) with 16300 ng/L, 9210 ng/L, 7220 ng/L, 6710 ng/L, and 4280 ng/L, respectively). Therefore, paracetamol had the highest concentrations in both INF and EFF.). A high concentration of paracetamol, 1100 μg/L was also detected in hospital effluents of Greek hospitals (Arvaniti et al., 2023) and 580 μg/L was found during an investigation performed on wastewater from hospitals in Kuwait (Mydlarczyk et al., 2022). Both these concentrations were above the maximum concentration of paracetamol found in this study (445 μg/L in INF). A comprehensive study performed on hospital wastewater in Greece revealed concentrations of diclofenac varied between 1.16 and 9.80 μg/L (Papageorgiou et al., 2019). These concentrations were in the same range as those found in this study, 2.93–8.95 μg/L. However, a study in Vietnam detected < 0.14–0.95 μg/L of diclofenac (Tran et al., 2014) and 3.84–6.74 μg/L of paracetamol from hospital wastewater effluents (Van Hoi et al., 2021) which concentrations were very low compared to those obtained from this study (paracetamol: 15–18 μg/L in EFF) suggesting variability in PPCPs concentrations from hospital effluents. Also, PPCPs concentration showed high variability for

some analytes in both INF and EFF The highest variations were noticed in INF for metoclopramide, sulfamethoxazole, abacavir, trimethoprim, and cimetidine (RSD 89.1%, 106%, 112%, 121%, and 128%, respectively). The high variability in concentrations of the latter PPCPs reflected differences in their usage, which in turn is a function of disease predominance. The average concentrations of each analyte are summarized in Table 1. The concentrations of PPCPs in all blanks were below LOQ. The raw data of PPCP concentrations in influents and effluents are summarized in an Excel sheet of Table S3 in the supplementary material.

3.2. Surface characterization

Data from DRIFTS analysis revealed that the absorption band from 1990 to 3500 cm^{-1} did not indicate any functional group for CH and BG materials see Fig. 1A. The spectra of the biochars for the three cookstoves showed similar trends. A peak corresponding to an aliphatic carbon functional group appeared at 3008 cm^{-1} for SW in the DRIFTS spectra with a broad stretching peak (Chen et al., 2008). An absorption bending band ranging between 1600 and 1560 cm^{-1} was detected for all biochars, which could represent C═C or C═O in aromatics, alkenes, ketones or aldehydes. The bending and broad peak at 1240 cm^{-1} for SW could indicate the presence of an ester. Peaks at 1030–1260 cm^{-1} for all biochars were assigned to functional groups C-C, C-O, C-N or C-X indicating, aromatic amine, ester or alkyl aryl ether. Peaks between 700 and 900 cm^{-1} indicated the presence of aromatic compounds, as suggested by (Keiluweit et al., 2010; Nandiyanto et al., 2019). The Raman analysis showed two main peaks at 1340 and 1590 cm^{-1}, representing aliphatic and aromatic carbon, respectively see Fig. 1B. See Table S4 and Table S5 in the Supplementary material for raw data from DRIFTS and Raman analyses respectively.

Results from XPS indicated that all samples had a relatively high carbon content, particularly the SW biochar as indicated in Table 2. This finding was supported by the high intensity of C-H peaks for aliphatic and aromatic compound functional groups present in the DRIFTS and Raman spectra (Fig. 1A & B). The oxygen content in SW was lower than in CH and BG, resulting in a lower average atomic ratio O/C for SW (0.07). Similarly, the average H/C ratio calculated from the Raman analysis data was in general lower for SW than for BG and CH, the highest value was 2.40 for biochar FCH. The H/C, O/C ratios, and percentage of carbon may be used to classify a carbonaceous material as biochar. The European Biochar Foundation (EBF) states that biochar should have $>$ 50% of C on a dry weight basis and an O/C ratio $<$ 0.4 (Klasson, 2017). Carbonaceous materials produced by cookstoves fulfilled these conditions. Furthermore, the H/C and O/C ratios may affect the adsorption of aromatic or nonpolar compounds (Nartey and Zhao, 2014; Parikh

Table 1
Average concentrations in ng/L of analyzed pharmaceuticals and personal care.

			INFLUENT				EFFLUENT			
Compound	LOQ	Group	Min (ng/L)	Max (ng/L)	Av (ng/L)	RSD (%)	Min (ng/L)	Max (ng/L)	Av (ng/L)	RSD (%)
Abacavir	9	ARV	3310	37300	14700	112	3240	5500	4220	21.7
Artemether	10	AMD	18.8	84.2	42.9	51.5	12.5	77.4	35.2	63.9
Artesunate	10	AMD	44.6	327	153	53.2	45	233	105	58.0
Atenolol	50	HD	183	286	245	17.1	74.2	129	97.4	21.1
Caffeine	30	S	17300	59700	38300	43.9	1900	2930	2260	15.6
Carbamazepine	50	P	<LOQ	<LOQ	<LOQ	-	63.7	76.8	70.2	7.20
Cimetidine	10	AUD	82.7	3880	1400	128	167	371	293	32.0
Ciprofloxacin	200	ATB	5160	15700	8730	57.8	3560	9040	6710	35.3
Clindamycin	50	ATB	21.1	63.1	47.3	40.7	448	865	690	26.7
Codeine	100	A	157	346	257	30.6	110	310	217	38.6
DBP	30	P	328	923	529	34.6	487	815	637	17.8
DEET	10	I	1220	2520	1730	29.4	574	886	686	19.4
Diazepam	20	P	<LOQ	69.0	33.8	88.6	40.3	58.0	47.8	13.5
Diclofenac	60	NSAID	2930	8950	4870	58.4	2930	4700	3630	20.6
Dihydroartemisinin	10	AM	34.2	208	105	58.2	54.9	204	116	46.3
Erythromycin	90	ATB	411	831	616	25.4	3250	9730	7220	38.8
Fluconazole	50	AM	159	211	184	9.6	439	920	703	27.5
Lamivudine	100	ARV	4090	13400	7560	52.5	1770	2230	1920	8.50
Levofloxacin	10	ATB	89.6	2530	1340	75.6	208	812	491	48.1
Lignocaine	100	LA	5040	24300	13100	56.6	8990	9630	9210	3.90
Lorazepam	50	P	318	952	569	42.7	73.3	249	138	38.7
Metoclopramide	60	GD	77.1	672	299	89.1	856	1980	1400	30.5
Metronidazole	30	ATB	3530	12700	7150	51.2	3030	4290	3470	12.4
Nevirapine	20	ARV	<LOQ	26.8	21.3	37.2	21.4	42.9	31.6	26.1
Paracetamol	10	NSAID	113000	445000	244000	58.3	15000	18000	16300	5.20
Sulfamethoxazole	50	ATB	461	4960	2000	106	758	1190	954	18.3
Tramadol	100	A	3020	5900	4160	30.4	2750	5970	4280	30.00
Trimethoprim	20	ATB	138	2810	1070	121	578	1600	1200	38.3

products in influent and effluent from CHUK wastewaters.
Influent (INF) was defined as wastewater that came directly from different services of the hospital, whereas effluent (EFF) was wastewater that left a WWTP of the hospital. Min, Max, and Av are the minimum, maximum, and average concentrations. RSD (in %) is the relative standard deviation between concentrations. LOQ is the limit of quantification. Av and RSD were calculated considering ½LOQ for all concentration values below LOQ. Abbreviations of therapy groups are defined in the text.

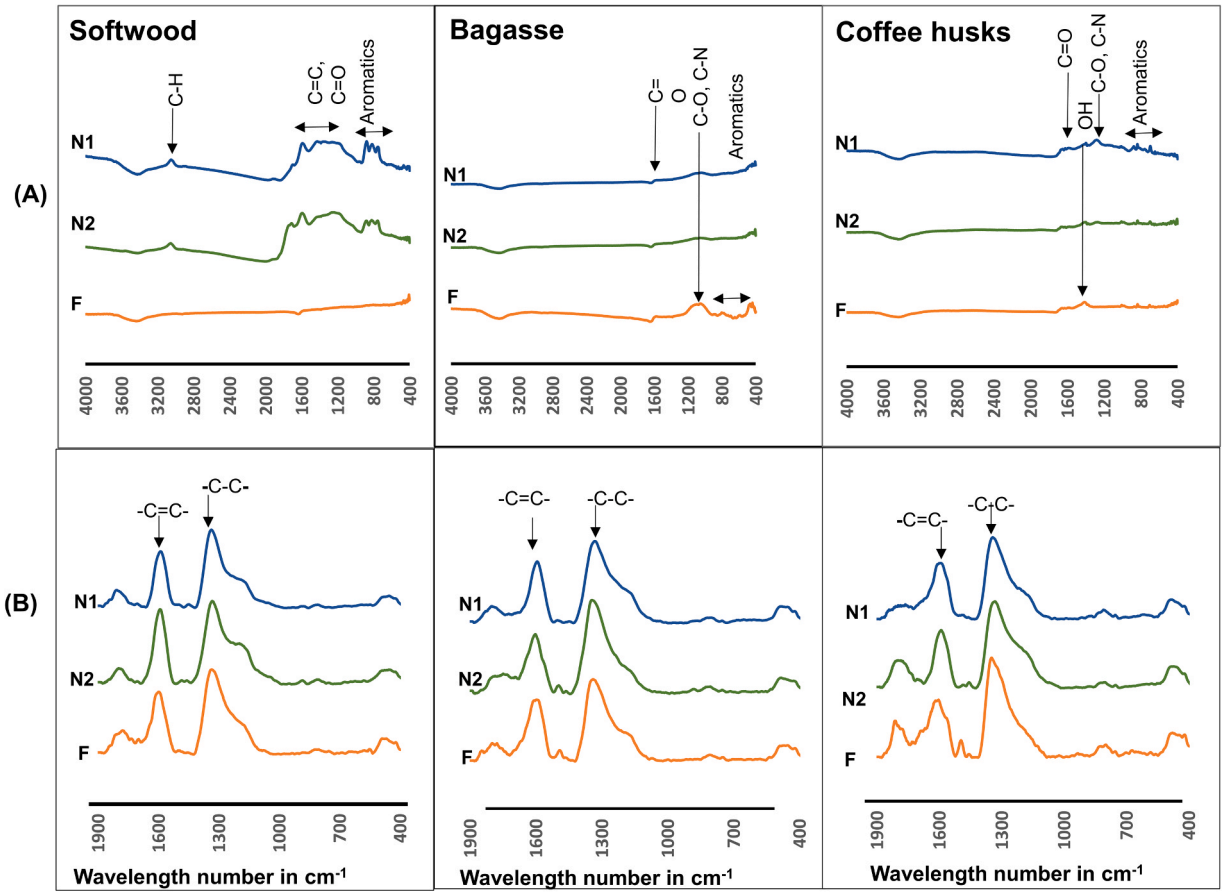

Fig. 1. Spectra from DRIFTS (A) and Raman (B). (A) shows chemical functional groups on the surface of all biochars produced by natural draft (N1), improved draft (N2) and forced draft gasifiers and for softwood, bagasse and coffee husks biomasses. (B) indicates intensities of aliphatic symbolized by –C-C- and aromatic, -C═C- groups.

Table 2
Atomic percentages of elements, BET surface area, and pore size of biochars.

Cookstove	Biochar	C	O	K	Ca	Si	Al	Traces	Surface area (m^2/g)	Pore size (nm)
	N1SW	90.4	9.6	-	-	-	-	-	213 ± 1.1	2.2 ± 0.7
N1	N1BG	90.3	8.5	-	traces	1.2	traces	Na, Fe	150 ± 1.4	2.5 ± 0.7
	N1CH	78.8	18.2	2.9	traces	-	-	Cl, N	-	-
	N2SW	90.9	8.7	0.5				Na, N	139 ± 0.9	2.6 ± 1.1
N2	N2BG	83.7	13.3	traces	traces	2.1	1	Na, Fe	116 ± 1.2	2.7 ± 0.9
	N2CH	80.9	14.2	4.9	traces			Cl	-	-
	FSW	90.5	8.1	1.4	traces	-	-	Na, Cl	289 ± 0.7	2.3 ± 0.6
F	FBG	81.6	14.2	-	traces	2.9	1.4	Na, Cl, Fe	175 ± 1.4	2.4 ± 0.5
	FCH	73.6	19.1	6	1.20	-	-	Na, Cl, P	57 ± 1.2	2.1 ± 0.8

Table 3
The H/C ratios calculated from Raman results and O/C calculated from the atomic percentage of C and O presented in Table 2.

Ratio	N1SW	N2SW	FSW	N1BG	N2BG	FBG	N1CH	N2CH	FCH
H/C	1.60	1.17	1.59	1.58	2.01	1.57	1.78	1.82	2.40
O/C	0.08	0.07	0.07	0.07	0.12	0.13	0.17	0.13	0.19

The H/C ratio was found by calculating the ratio between the intensity of the aliphatic C band and the intensity of the aromatic band for each biochar from Raman Spectroscopy analysis. The O/C ratio was calculated using the following formula O/C= (%O: Mo)/(%C: Mc)] with Mo and Mc atomic mass of oxygen and carbon respectively. The %O and %C were provided by XPS analysis.

et al., 2014; Xiao et al., 2016). The high H/C ratio may increase the polarity of the biochar, increasing its hydrophilic properties (Klasson, 2017; Mukome et al., 2013) and capacity for heavy metal removal (Ok et al., 2015). The calculated values of H/C and O/C are indicated in Table 3. Among the individual biochars, N2SW, FSW, and N1BG had the same O/C ratio (0.07). N1SW, FSW, N1BG and FBG exhibited almost similar H/C atomic ratios. Furthermore, these four biochars exhibited relatively highest surface areas, as indicated by BET analysis, with the highest area of 289 m^2/g shown by FSW. However, the corresponding pore sizes were small and relatively the same for all biochars as shown in Table 2.

The presence of K and Ca was noteworthy in the CH samples, a high K content in coffee residues has been previously reported (Tombarkiewicz et al., 2022; Tsai et al., 2012; Zoca et al., 2014). Aluminum (Al) and Silicon (Si) were only present in the BG samples. The presence of Si in bagasse was consistent with various publications (Ameram et al., 2019; Bortolotto Teixeira et al., 2021; Norsuraya et al., 2016) and Ca has been found with a relatively high percentage during the determination of the chemical composition of sugarcane bagasse biochar at different pyrolysis temperatures (Moradi-Choghamarani et al., 2019).

3.3. Removal efficiency of biochars

The detected and quantified PPCP presented different degrees of adsorption by biochars. The sum of PPCP before and after adsorption experiments showed that the RR averages of biochars varied between 14.2% and 65.5% for the least and the most performing respectively. Fourteen PPCPs were at least removed by one of the top five biochars that are N1BG, FSW, FBG, N1SW and, N2SW with RRs greater than 50% as shown in Fig. 2. The RRs of all PPCPs for all nine biochars are represented in Table S6 of Supplementary materials. Metoclopramide was removed with RR> 95% by biochars N1BG, FSW, and FBG, and both metoclopramide and diazepam were removed by all biochars with RR> 56.6%. Cimetidine, lignocaine, and, tramadol were removed with RR> 80.5% by N1BG and FSW, the same RR was also observed for caffeine. Antibiotics; ciprofloxacin, clindamycin, erythromycin, levofloxacin, and trimethoprim, had RRs ranging between 54.4% and 93.3%, removals performed by N1BG, FSW, and FBG. Good removal rates of antibiotics by biochars were also reported in various studies (Afzal et al., 2018; Du et al., 2022; Zhao et al., 2019a). For example, biochar made from guayule bagasse removed erythromycin with RR varying between 50% and 74% (Ndoun et al., 2021) being in the same range as results obtained in this study using FSW, FBG, and N1BG biochars (with RRs of 54.4, 67,3% and 87.1% respectively) for the same antibiotic. However, the latter biochars removed metronidazole and sulfamethoxazole with RRs varied between 25.9% and 43.6%. These results were in the same range as that reported during the investigation study on the adsorption of sulfamethoxazole from aqueous solution using carbon nanotubes, 30%; in the same study, the RR became > 70% using carbon nanotubes modified by ionic liquids (Lawal et al., 2018). The N1BG and FSW biochars adsorbed the detected NSAIDs, diclofenac, and paracetamol at 73.7–77.5% respectively. Artesunate was not detectably removed by any of the 9 biochars. Although the biochars having the high RR in this study, generally are those having the highest surface areas as indicated by results from BET and the calculated RR presented in Table S6, the correlation between the surface area and RR was not clear; for example, N1BG and FSW which were the top 2 biochars had different surface areas, 150 ± 1.4 and 289 ± 0.7 m^2/g respectively suggesting that the surface area was not the only main driving force of adsorption of PPCPs on biochars used in this study. This observation is consistent with that reported during the adsorption of heavy metals using sugarcane bagasse biochar and activated carbon, the surface area of the latter was higher than that of biochar, but

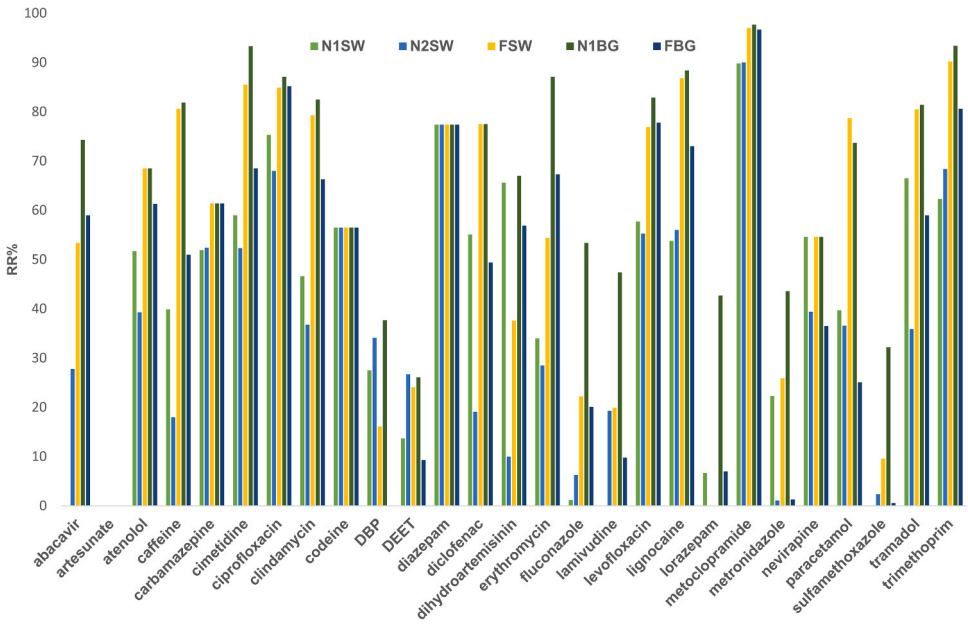

Fig. 2. Frequencies in removal rates in the percentage of pharmaceuticals and personal care products by the top five biochars, namely N1SW, N2SW, FSW, N1BG, and FBG.

its sorption capacity was low compared to the biochar (Mohan et al., 2014). Another study on removal of dyes argued that the biochar surface area played a role in adsorption but the charge of biochar might govern that adsorption (Peterson et al., 2021). Interactions between biochars and PPCPs involve several physicochemical mechanisms. In this study, DRIFTS and Raman showed that biochars were rich in aromatic and aliphatic carbon which are known to contain excess π –electrons facilitating π-π or donor-acceptor interactions with molecules having O, N, P, Cl, and S atoms dedicated to have deficit in electrons (Vithanage et al., 2017). Biochars can also interact with analytes by van der Waals forces, dipole-dipole forces, pore filling, etc. In addition to C, O, and H, XPS analysis demonstrated the presence of mineral elements like K, Ca, Si, Al, etc. These elements could interact with polar compounds with H bonds which are stronger attractions than van der Waals (Guo et al., 2020), in addition biochars from coffee husks contained O-H group which might participates in H bonding reactions as well. Yet, the most relevant interactions that might explain the extreme removal rates of certain PPCP were not clear in this study. Additional parameters like the charge on the biochar surface indicating electrostatic attractions that could occur, the organic and ash contents informing on the partition capacity of biochars (Zhao et al., 2019b), the surface structure of biochars, etc. need also to be investigated to figure out the main characteristics causing such differences in RRs.

An alternative way to estimate the efficiencies of biochars is to compare the removal rates of relevant chemicals, i.e. apply a "weighted" value based on the priority of the individual compounds. In an earlier paper, the concept of a critical effect concentration (CEC) of a pharmaceutical was introduced (Fick et al., 2010). This is an estimated water concentration, based on the potency and log K_{ow} of each pollutant, at which aquatic wildlife may be affected. CEC is based on the major assumption that functionally conserved drug targets and that human therapeutic plasma concentrations (HTPC) can be compared with a measured, or theoretically predicted, fish steady-state plasma concentration (FSSPC). If the FSSPC is higher than the HTPC, i.e. ratio between them is above one, then the concentration in the exposed fish is likely to induce a pharmacological response in humans. Additional information regarding the CEC concept, conserved drug targets, theoretical background and calculations are presented in a previous paper (Fick et al., 2010). Ranking chemicals based on the ratio between measured water concentrations and their estimated CEC value would be one possible way forward to take into account the vast differences in potencies and physicochemical properties between different chemicals, and facilitate the identification of chemicals of environmental concern. Dividing the measured concentration (C) by the individual CEC value for each pharmaceutical will give an estimate of the effect ratio (ER) (see Eq. 2). An effect ratio ≥ 1 indicated that the measured pharmaceutical was at a concentration likely to cause an effect.

$$\frac{\text{Measured level}}{\text{CEC}} = \textit{Effect} \quad \textit{ratio} \tag{2}$$

Calculations of the treated effluent based on Eq. 2 showed that the majority of the pharmaceuticals had a low effect ratio and only a few had a high. The top 5 pharmaceuticals having the highest ER were; diclofenac, tramadol, lorazepam, metoclopramide, and lignocaine with ER of 0.65; 0.59; 0.07; 0.04 and, 0.02 respectively. By comparing the sum of the effect ratios before and after the adsorption, biochars removing the most relevant pharmaceuticals were provided. This study showed that N1BG and FSW were the most effective for removing pharmaceuticals with high effect ratios; they removed 78.3% and 75.4% respectively of the sum of effect ratios as indicated in Table 4. Table S7 in Supplementary materials shows the effect ratios of all detected pharmaceuticals.

Considering biochars produced by the cookstove N1 (N1SW, N1BG, and N1CH), 96.3% of the analyzed PPCPs exhibited a significant difference ($p < 0.05$) in RR, similarly biochars produced by the cookstoves F and N2 (FSW, FBG, FCH and N2SW, N2BG, N2CH), this comparison of RR revealed that 74.0% and 55.5% of PPCPs respectively presented a significant difference as illustrated by Fig. 3A. These results showed that the type of feedstock or biomass considered to produce biochar matters. Similarly, considering biochars produced from one type of feedstock by different cookstoves, more than 85% of PPCPs revealed a significant difference in their removals, suggesting that the conditions under which biochars are produced matter as indicated in Fig. 3B. These findings agreed with studies arguing that the type of feedstock and technologies used to produce biochars, (types of furnaces, pyrolysis temperatures, types of feedstock, etc.) affect their properties (Ferraro et al., 2021; Mukome et al., 2013; Qambrani et al., 2017; Tomczyk et al., 2020) and influence their adsorption capacities (Ambaye et al., 2021; Ghodake et al., 2021; Rutherford et al., 2012). The calculated p values for biochars produced by the same cookstoves and those produced from the same feedstock are presented in the supplementary material in Tables S8A and S8B.

4. Conclusion

Biochars produced by cookstoves removed PPCP at different degrees. Some, e.g., N1BG and FSW, were more effective at removal than others, e.g., N2CH. Chemicals like metoclopramide and diazepam were highly adsorbed by all biochars with RRs ranging between 56.6% and 97.7%, whereas artesunate was not adsorbed. Significant differences were detected in removal rates among the biochars from the same cookstoves and also from the same feedstock, as shown by p-values. Further studies on biochar characterization are needed to identify the main parameters explaining such differences.

CRediT authorship contribution statement

B. Mukarunyana: Methodology, Validation, Formal analysis, Investigation, Writing – original draft. **C. Boman:** Conceptualization, Resources, Writing – review & editing. **T. Kabera:** Writing – review & editing. **R. Lindgren:** Investigation, Writing – review & editing. **J. Fick:** Conceptualization, Methodology, Investigation, Resources, Writing – review & editing.

Table 4
Critical effect concentrations and effect ratio of the top 5 pharmaceuticals before and after application of biochars.

Pharmaceutical	CEC (ng/L)	Effect ratio before and after adsorption of PPCPs on biochars									
		EFF1	NSW	NBG	NCH	INSW	INBG	INCH	FSW	FBG	FCH
Diclofenac	4560	0.65	0.29	0.15	0.52	0.53	0.57	0.65	0.15	0.33	0.29
Tramadol	4800	0.59	0.20	0.11	0.50	0.38	0.59	0.59	0.12	0.24	0.24
Lorazepam	2650	0.07	0.07	0.04	0.07	0.07	0.07	0.07	0.07	0.07	0.07
Metoclopramide	22,100	0.04	0.00	0.00	0.00	0.00	0.00	0.00	0.00	0.00	0.00
Lignocaine	467,000	0.02	0.01	0.00	0.02	0.01	0.02	0.02	0.00	0.01	0.01
SUM		1.38	0.57	0.30	1.12	0.99	1.26	1.34	0.34	0.65	0.61

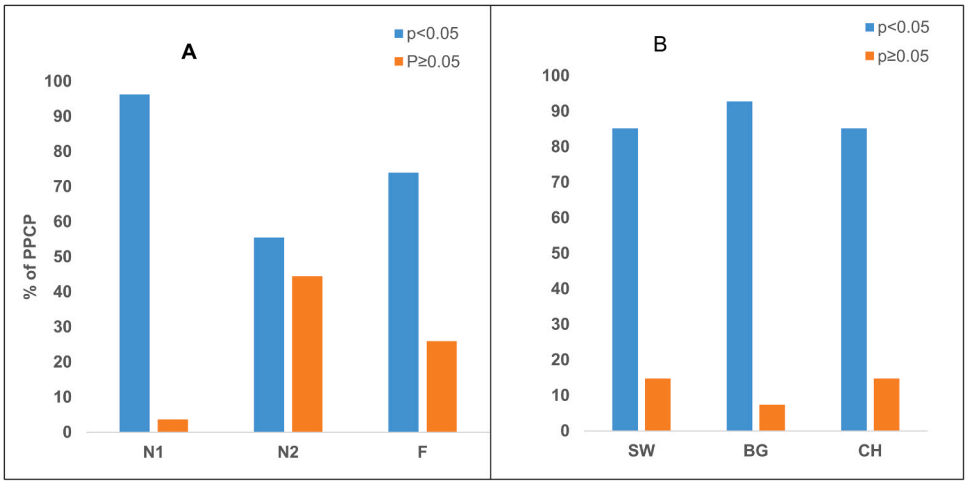

Fig. 3. Plots of *p*-values calculated using ANOVA to compare the removal rates of PPCP by biochars produced by one type of cookstove (Figure A); and to compare the removal rates of PPCP by biochars from one type of feedstock (Figure B). The level of significance was set at 0.05.

Declaration of Competing Interest

The authors declare that they have no known competing financial interests or personal relationships that could have appeared to influence the work reported in this paper.

Data Availability

Data will be made available on request.

Acknowledgement

The authors would like to thank the University Teaching Hospital of Kigali (CHUK) leaders especially the Ethics Committee for approving sampling effluents from the wastewater treatment plant of the hospital. The support of the Swedish International Development Agency (SIDA) is also acknowledged.

Appendix A. Supporting information

Supplementary data associated with this article can be found in the online version at doi:10.1016/j.eti.2023.103391.

References

Afzal, M.Z., Sun, X.-F., Liu, J., Song, C., Wang, S.-G., Javed, A., 2018. Enhancement of ciprofloxacin sorption on chitosan/biochar hydrogel beads. Sci. Total Environ. 639, 560–569.

Al-Maadheed, S., Goktepe, I., Latiff, A.B.A., Shomar, B., 2019. Antibiotics in hospital effluent and domestic wastewater treatment plants in Doha, Qatar. J. Water Process Eng. 28, 60–68.

Ambaye, T.G., Vaccari, M., Van Hullebusch, E.D., Amrane, A., Rtimi, S., 2021. Mechanisms and adsorption capacities of biochar for the removal of organic and inorganic pollutants from industrial wastewater. Int. J. Environ. Sci. Technol. 18 (10), 3273–3294. https://doi.org/10.1007/s13762-020-03060-w.

Ameram, N., Muhammad, S., Yusof, N.A.A.N., Ishak, S., Ali, A., Shoparwe, N.F., Ter, T.P., 2019. Chemical composition in sugarcane bagasse: delignification with sodium hydroxide. Malays. J. Fundam. Appl. Sci. 15 (2), 232–236.
Antal, M.J., Grønli, M., 2003. The art, science, and technology of charcoal production. Ind. Eng. Chem. Res. 42 (8), 1619–1640.
Arvaniti, O., Arvaniti, E., Gyparakis, S., Sabathianakis, I., Karagiannis, E., Pettas, E., Gkotsis, G., Nika, M., Thomaidis, N., Manios, T., 2023. Occurrence of pharmaceuticals in the wastewater of a Greek hospital: combining consumption data collection and LC-QTOF-MS analysis. Sci. Total Environ. 858, 160153.
Aydin, S., Aydin, M.E., Ulvi, A., Kilic, H., 2019. Antibiotics in hospital effluents: occurrence, contribution to urban wastewater, removal in a wastewater treatment plant, and environmental risk assessment. Environ. Sci. Pollut. Res. 26 (1), 544–558. https://doi.org/10.1007/s11356-018-3563-0.
Azuma, T., Otomo, K., Kunitou, M., Shimizu, M., Hosomaru, K., Mikata, S., Ishida, M., Hisamatsu, K., Yunoki, A., Mino, Y., 2019. Environmental fate of pharmaceutical compounds and antimicrobial-resistant bacteria in hospital effluents, and contributions to pollutant loads in the surface waters in Japan. Sci. Total Environ. 657, 476–484.
Bahamon, D., Vega, L.F., 2017. Pharmaceuticals removal from water effluents by adsorption in activated carbons using Monte Carlo simulations. In: Computer Aided Chemical Engineering, Vol. 40. Elsevier, pp. 2695–2700.
Bortolotto Teixeira, L., de Moraes, Guzi, Paolinelli Shinhe, E., Falk, G., G, Novaes de Oliveira, A.P., 2021. Obtaining biogenic silica from sugarcane bagasse and leaf ash. Waste Biomass Valoriz. 12, 3205–3221.
Chauhan, S., Shafi, T., Dubey, B.K., Chowdhury, S., 2022. Biochar-mediated removal of pharmaceutical compounds from aqueous matrices via adsorption. Waste Dispos. Sustain. Energy 1–26.
Chen, B., Zhou, D., Zhu, L., 2008. Transitional adsorption and partition of nonpolar and polar aromatic contaminants by biochars of pine needles with different pyrolytic temperatures. Environ. Sci. Technol. 42 (14), 5137–5143.
Cukierman, A.L., Nunell, G.V., Bonelli, P.R., 2019. Removal of emerging pollutants from water through adsorption onto carbon-based materials. Emerging and Nanomaterial Contaminants in Wastewater. Elsevier, pp. 159–213.
Deguenon, E., Dougnon, V., Houssou, V.M.C., Gbotche, E., Ahoyo, R.A., Fabiyi, K., Agbankpe, J., Mousse, W., Lougbegnon, C., Klotoe, J.R., 2022. Hospital effluents as sources of antibiotics residues, resistant bacteria and heavy metals in Benin. SN Appl. Sci. 4 (8), 206.
Domingues, R.R., Trugilho, P.F., Silva, C.A., de Melo, I.C.N., Melo, L.C., Magriotis, Z.M., Sanchez-Monedero, M.A., 2017. Properties of biochar derived from wood and high-nutrient biomasses with the aim of agronomic and environmental benefits. PloS One 12 (5), e0176884.
Du, L., Ahmad, S., Liu, L., Wang, L., Tang, J., 2022. A review of antibiotics and antibiotic resistance genes (ARGs) adsorption by biochar and modified biochar in water. Sci. Total Environ., 159815
Duku, M.H., Gu, S., Hagan, E.B., 2011. Biochar production potential in Ghana—a review. Renew. Sustain. Energy Rev. 15 (8), 3539–3551. https://doi.org/10.1016/j.rser.2011.05.010.
Fekadu, S., Alemayehu, E., Dewil, R., Van Der Bruggen, B., 2019. Pharmaceuticals in freshwater aquatic environments: a comparison of the African and European challenge. Sci. Total Environ. 654, 324–337. https://doi.org/10.1016/j.scitotenv.2018.11.072.
Ferraro, G., Pecori, G., Rosi, L., Bettucci, L., Fratini, E., Casini, D., Rizzo, A.M., Chiaramonti, D., 2021. Biochar from lab-scale pyrolysis: influence of feedstock and operational temperature. Biomass Convers. Biorefinery. https://doi.org/10.1007/s13399-021-01303-5.
Fick, J., Lindberg, R.H., Tysklind, M., Larsson, D.J., 2010. Predicted critical environmental concentrations for 500 pharmaceuticals. Regul. Toxicol. Pharmacol. 58 (3), 516–523.
Gao, F., Xue, Y., Deng, P., Cheng, X., Yang, K., 2015. Removal of aqueous ammonium by biochars derived from agricultural residuals at different pyrolysis temperatures. Chem. Speciat. Bioavailab. 27 (2), 92–97.
Ghodake, G.S., Shinde, S.K., Kadam, A.A., Saratale, R.G., Saratale, G.D., Kumar, M., Palem, R.R., AL-Shwaiman, H.A., Elgorban, A.M., Syed, A., 2021. Review on biomass feedstocks, pyrolysis mechanism and physicochemical properties of biochar: state-of-the-art framework to speed up vision of circular bioeconomy. J. Clean. Prod. 297, 126645.
Gorzsás, A., Sundberg, B., 2014. Chemical fingerprinting of arabidopsis using fourier transform infrared (FT-IR) spectroscopic approaches. Arabidopsis Protocols. Springer, pp. 317–352.
Guo, M., Song, W., Tian, J., 2020. Biochar-facilitated soil remediation: mechanisms and efficacy variations. Front. Environ. Sci. 183.
Ippolito, J.A., Cui, L., Kammann, C., Wrage-Mönnig, N., Estavillo, J.M., Fuertes-Mendizabal, T., Cayuela, M.L., Sigua, G., Novak, J., Spokas, K., Borchard, N., 2020. Feedstock choice, pyrolysis temperature and type influence biochar characteristics: a comprehensive meta-data analysis review. Biochar 2 (4), 421–438. https://doi.org/10.1007/s42773-020-00067-x.
Keiluweit, M., Nico, P.S., Johnson, M.G., Kleber, M., 2010. Dynamic molecular structure of plant biomass-derived black carbon (biochar). Environ. Sci. Technol. 44 (4), 1247–1253.
Kim, H., Ko, R.-A., Lee, S., Chon, K., 2020. Removal efficiencies of manganese and iron using pristine and phosphoric acid pre-treated biochars made from banana peels. Water 12 (4), 1173. https://doi.org/10.3390/w12041173.
Klasson, K.T., 2017. Biochar characterization and a method for estimating biochar quality from proximate analysis results. Biomass Bioenergy 96, 50–58.
Lawal, I.A., Lawal, M.M., Akpotu, S.O., Azeez, M.A., Ndungu, P., Moodley, B., 2018. Theoretical and experimental adsorption studies of sulfamethoxazole and ketoprofen on synthesized ionic liquids modified CNTs. Ecotoxicol. Environ. Saf. 161, 542–552.
López-Cano, I., Cayuela, M., Mondini, C., Takaya, C., Ross, A., Sánchez-Monedero, M., 2018. Suitability of different agricultural and urban organic wastes as feedstocks for the production of biochar—Part 1: physicochemical characterisation. Sustainability 10 (7), 2265.
Melvin, S.D., Leusch, F.D., 2016. Removal of trace organic contaminants from domestic wastewater: a meta-analysis comparison of sewage treatment technologies. Environ. Int. 92, 183–188.
Mohan, D., Rajput, S., Singh, V.K., Steele, P.H., Pittman Jr, C.U., 2011. Modeling and evaluation of chromium remediation from water using low cost bio-char, a green adsorbent. J. Hazard. Mater. 188 (1–3), 319–333.
Mohan, D., Sarswat, A., Ok, Y.S., Pittman Jr., C.U., 2014. Organic and inorganic contaminants removal from water with biochar, a renewable, low cost and sustainable adsorbent–a critical review. Bioresour. Technol. 160, 191–202. https://doi.org/10.1016/j.biortech.2014.01.120.
Mojiri, A., Baharlooeian, M., Kazeroon, R.A., Farraji, H., Lou, Z., 2020. Removal of pharmaceutical micropollutants with integrated biochar and marine microalgae. Microorganisms 9 (1), 4. https://doi.org/10.3390/microorganisms9010004.
Moradi-Choghamarani, F., Moosavi, A.A., Baghernejad, M., 2019. Determining organo-chemical composition of sugarcane bagasse-derived biochar as a function of pyrolysis temperature using proximate and Fourier transform infrared analyses. J. Therm. Anal. Calorim. 138 (1), 331–342. https://doi.org/10.1007/s10973-019-08186-9.
Mukome, F.N.D., Zhang, X., Silva, L.C.R., Six, J., Parikh, S.J., 2013. Use of chemical and physical characteristics to investigate trends in biochar feedstocks. J. Agric. Food Chem. 61 (9), 2196–2204. https://doi.org/10.1021/jf3049142.
Mydlarczyk, A., Al-Haddad, A., Abdullah, H., Aba, A., Esmaeel, A., Al-Yaseen, R., 2022. Investigations on pharmaceuticals and radioactive elements in wastewater from hospitals in Kuwait. Desalination Water Treat. 263, 145–151.
Naderi, M., 2015. Surface area: brunauer–emmett–teller (BET). Progress in Filtration and Separation. Elsevier, pp. 585–608.
Nandiyanto, A.B.D., Oktiani, R., Ragadhita, R., 2019. How to read and interpret FTIR spectroscope of organic material. Indones. J. Sci. Technol. 4 (1), 97–118.
Nartey, O.D., Zhao, B., 2014. Biochar preparation, characterization, and adsorptive capacity and its effect on bioavailability of contaminants: an overview. Adv. Mater. Sci. Eng. *2014*.
Ndoun, M.C., Elliott, H.A., Preisendanz, H.E., Williams, C.F., Knopf, A., Watson, J.E., 2021. Adsorption of pharmaceuticals from aqueous solutions using biochar derived from cotton gin waste and guayule bagasse. Biochar 3, 89–104.
Norsuraya, S., Fazlena, H., Norhasyimi, R., 2016. Sugarcane bagasse as a renewable source of silica to synthesize Santa Barbara Amorphous-15 (SBA-15). Procedia Eng. 148, 839–846.
OECD. (2019). Pharmaceutical Residues in Freshwater: Hazards and Policy Responses. In: Organisation for Economic Cooperation and Development Paris, France.
Ok, Y.S., Uchimiya, S.M., Chang, S.X., Bolan, N., 2015. Biochar: Production, Characterization, and Applications. CRC Press.

Papageorgiou, M., Zioris, I., Danis, T., Bikiaris, D., Lambropoulou, D., 2019. Comprehensive investigation of a wide range of pharmaceuticals and personal care products in urban and hospital wastewaters in Greece. Sci. Total Environ. 694, 133565.
Parikh, S.J., Goyne, K.W., Margenot, A.J., Mukome, F.N., Calderón, F.J., 2014. Soil chemical insights provided through vibrational spectroscopy. In: Advances in agronomy, Vol. 126. Elsevier, pp. 1–148.
Patel, M., Kumar, R., Kishor, K., Mlsna, T., Pittman Jr, C.U., Mohan, D., 2019. Pharmaceuticals of emerging concern in aquatic systems: chemistry, occurrence, effects, and removal methods. Chem. Rev. 119 (6), 3510–3673.
Patel, M., Kumar, R., Pittman, C.U., Mohan, D., 2021. Ciprofloxacin and acetaminophen sorption onto banana peel biochars: environmental and process parameter influences. Environ. Res. 201, 111218 https://doi.org/10.1016/j.envres.2021.111218.
Peterson, S., Kim, S., & Adkins, J. (2021). Surface Charge Effects on Adsorption of Solutes by Poplar and Elm Biochars. C 2021, 7, 11. In: s Note: MDPI stays neutral with regard to jurisdictional claims in published.
Piel, S., Blondeau, S., Pérot, J., Baurès, E., Thomas, O., 2013. Pharmaceutical removal by the activated carbon process. Water Qual. Res. J. Can. 48 (2), 121–132.
Posadas, E., Bochon, S., Coca, M., García-González, M., García-Encina, P., Muñoz, R., 2014. Microalgae-based agro-industrial wastewater treatment: a preliminary screening of biodegradability. J. Appl. Phycol. 26 (6), 2335–2345.
Qambrani, N.A., Rahman, M.M., Won, S., Shim, S., Ra, C., 2017. Biochar properties and eco-friendly applications for climate change mitigation, waste management, and wastewater treatment: a review. Renew. Sustain. Energy Rev. 79, 255–273. https://doi.org/10.1016/j.rser.2017.05.057.
Qiu, B., Tao, X., Wang, H., Li, W., Ding, X., Chu, H., 2021. Biochar as a low-cost adsorbent for aqueous heavy metal removal: a review. J. Anal. Appl. Pyrolysis 155, 105081.
Ram, S.K., Panidepu, H., Cheernam, V., Tyagi, R.D., 2020. Pharmaceutical metabolites and their by-products in hospital wastewater. Curr. Dev. Biotechnol. Bioeng. 43–78. https://doi.org/10.1016/b978-0-12-819722-6.00002-x.
Reis, E.O., Foureaux, A.F.S., Rodrigues, J.S., Moreira, V.R., Lebron, Y.A.R., Santos, L.V.S., Amaral, M.C.S., Lange, L.C., 2019. Occurrence, removal and seasonal variation of pharmaceuticals in Brasilian drinking water treatment plants. Environ. Pollut. 250, 773–781. https://doi.org/10.1016/j.envpol.2019.04.102.
Rutherford, D.W., Wershaw, R.L., Rostad, C.E., Kelly, C.N., 2012. Effect of formation conditions on biochars: compositional and structural properties of cellulose, lignin, and pine biochars. Biomass Bioenergy 46, 693–701. https://doi.org/10.1016/j.biombioe.2012.06.026.
Santos, L.H., Gros, M., Rodriguez-Mozaz, S., Delerue-Matos, C., Pena, A., Barceló, D., Montenegro, M.C.B., 2013. Contribution of hospital effluents to the load of pharmaceuticals in urban wastewaters: identification of ecologically relevant pharmaceuticals. Sci. Total Environ. 461, 302–316.
Schwendicke, F., Stolpe, M., Innes, N., 2016. Conventional treatment, hall technique or immediate pulpotomy for carious primary molars: a cost-effectiveness analysis. Int. Endod. J. 49 (9), 817–826.
Shin, J., Lee, Y.-G., Lee, S.-H., Kim, S., Ochir, D., Park, Y., Kim, J., Chon, K., 2020. Single and competitive adsorptions of micropollutants using pristine and alkali-modified biochars from spent coffee grounds. J. Hazard. Mater. 400, 123102 https://doi.org/10.1016/j.jhazmat.2020.123102.
Shin, J., Kwak, J., Lee, Y.-G., Kim, S., Choi, M., Bae, S., Lee, S.-H., Park, Y., Chon, K., 2021. Competitive adsorption of pharmaceuticals in lake water and wastewater effluent by pristine and NaOH-activated biochars from spent coffee wastes: contribution of hydrophobic and π-π interactions. Environ. Pollut. 270, 116244 https://doi.org/10.1016/j.envpol.2020.116244.
Skoulou, V., Koufodimos, G., Samaras, Z., Zabaniotou, A., 2008. Low-temperature gasification of olive kernels in a 5-kW fluidized bed reactor for H2-rich producer gas. Int. J. Hydrog. Energy 33 (22), 6515–6524.
Sundberg, C., Karltun, E., Gitau, J.K., Kätterer, T., Kimutai, G.M., Mahmoud, Y., Njenga, M., Nyberg, G., Roing de Nowina, K., Roobroeck, D., 2020. Biochar from cookstoves reduces greenhouse gas emissions from smallholder farms in Africa. Mitig. Adapt. Strateg. Glob. Change 25, 953–967.
Thommes, M., Kaneko, K., Neimark, A.V., Olivier, J.P., Rodriguez-Reinoso, F., Rouquerol, J., Sing, K.S., 2015. Physisorption of gases, with special reference to the evaluation of surface area and pore size distribution (IUPAC Technical Report). Pure Appl. Chem. 87 (9–10), 1051–1069.
Tombarkiewicz, B., Antonkiewicz, J., Lis, M.W., Pawlak, K., Trela, M., Witkowicz, R., Gorczyca, O., 2022. Chemical properties of the coffee grounds and poultry eggshells mixture in terms of soil improver. Sci. Rep. 12 (1), 2592.
Tomczyk, A., Sokołowska, Z., Boguta, P., 2020. Biochar physicochemical properties: pyrolysis temperature and feedstock kind effects. Rev. Environ. Sci. Bio/Technol. 19 (1), 191–215. https://doi.org/10.1007/s11157-020-09523-3.
Tran, N.H., Urase, T., Ta, T.T., 2014. A preliminary study on the occurrence of pharmaceutically active compounds in hospital wastewater and surface water in Hanoi, Vietnam. CLEAN–Soil Air Water 42 (3), 267–275.
Tsai, W.-T., Liu, S.-C., Hsieh, C.-H., 2012. Preparation and fuel properties of biochars from the pyrolysis of exhausted coffee residue. J. Anal. Appl. Pyrolysis 93, 63–67. https://doi.org/10.1016/j.jaap.2011.09.010.
Van Hoi, B., Vu, C.-T., Phung-Thi, L.-A., Thi Nguyen, T., Nguyen, P.T., Mai, H., Le, P.-T., Nguyen, T.-H., Thanh Duong, D., Nguyen Thi, H., 2021. Determination of pharmaceutical residues by UPLC-MS/MS method: validation and application on surface water and hospital wastewater. J. Anal. Methods Chem. *2021*.
Vaudreuil, M.-A., Duy, S.V., Munoz, G., Sauvé, S., 2022. Pharmaceutical pollution of hospital effluents and municipal wastewaters of Eastern Canada. Sci. Total Environ. 846, 157353.
Vithanage, M., Herath, I., Almaroai, Y.A., Rajapaksha, A.U., Huang, L., Sung, J.-K., Lee, S.S., Ok, Y.S., 2017. Effects of carbon nanotube and biochar on bioavailability of Pb, Cu and Sb in multi-metal contaminated soil. Environ. Geochem. Health 39, 1409–1420.
Wilkinson, J.L., Boxall, A.B., Kolpin, D.W., Leung, K.M., Lai, R.W., Galbán-Malagón, C., Adell, A.D., Mondon, J., Metian, M., Marchant, R.A., 2022. Pharmaceutical pollution of the world's rivers. Proc. Natl. Acad. Sci. 119 (8), e2113947119.
Xiao, X., Chen, Z., Chen, B., 2016. H/C atomic ratio as a smart linkage between pyrolytic temperatures, aromatic clusters and sorption properties of biochars derived from diverse precursory materials. Sci. Rep. 6 (1), 1–13.
Zhang, X., Yan, S., Chen, J., Tyagi, R., Li, J., 2020. Physical, chemical, and biological impact (hazard) of hospital wastewater on the environment: presence of pharmaceuticals, pathogens, and antibiotic-resistance genes. Current Developments in Biotechnology and Bioengineering. Elsevier,, pp. 79–102.
Zhao, J., Liang, G., Zhang, X., Cai, X., Li, R., Xie, X., Wang, Z., 2019. Coating magnetic biochar with humic acid for high efficient removal of fluoroquinolone antibiotics in water. Sci. Total Environ. 688, 1205–1215.
Zhao, Z., Wu, Q., Nie, T., Zhou, W., 2019b. Quantitative evaluation of relationships between adsorption and partition of atrazine in biochar-amended soils with biochar characteristics. RSC Adv. 9, 4162–4171.
Zoca, S.M., Penn, C.J., Rosolem, C.A., Alves, A.R., Neto, L.O., Martins, M.M., 2014. Coffee processing residues as a soil potassium amendment. Int. J. Recycl. Org. Waste Agric. 3, 155–165.